Supporting Information for: Nanoparticle Taylor dispersion near charged surfaces with an open boundary

Alexandre Vilquin,[1,2,*] Vincent Bertin,[1,3,4,*] Elie Raphaël,[1,2] David S. Dean,[3,5] Thomas Salez,[3,†] and Joshua D. McGraw[1,2,‡]

[1] *Gulliver CNRS UMR 7083, PSL Research University, ESPCI Paris, 10 rue Vauquelin, 75005 Paris, France*
[2] *IPGG, 6 rue Jean-Calvin, 75005 Paris, France*
[3] *Univ. Bordeaux, CNRS, LOMA, UMR 5798, F-33405, Talence, France*
[4] *Physics of Fluids Group, Faculty of Science and Technology, and Mesa+ Institute, University of Twente, 7500AE Enschede, The Netherlands.*
[5] *Team MONC, INRIA Bordeaux Sud Ouest, CNRS UMR 5251, Bordeaux INP, Univ. Bordeaux, F-33400, Talence, France.*

(Dated: May 22, 2022)

* The authors contributed equally
† thomas.salez@cnrs.fr
‡ joshua.mcgraw@cnrs.fr

MOMENT THEORY

A. Advection-diffusion model

We suppose a dilute suspension of spherical nanoparticles of radius a, flowing in a 2d (xz) channel where x is the streamwise direction. A rigid wall is located at $z = 0$, with a no-slip condition. The nanoparticles are submitted to electrostatic interactions, which generate an external force $-U'_{\rm el}(z)$ on the particle, where $U_{\rm el}$ is a Debye-Hückel energy potential defined in Eq.(1) of the main text. The center-of-mass position of the nanoparticles can be described in terms of concentration field, denoted $c(x, z, t)$, and which follows the Fokker-Planck equation

$$\frac{\partial c}{\partial t} + v_x(z)\frac{\partial c}{\partial x} = D_x(z)\frac{\partial^2 c}{\partial x^2} + \frac{\partial}{\partial z}\left(D_z(z)\left[\frac{\partial c}{\partial z} + \frac{U'_{\rm el}(z)}{kT}c\right]\right), \tag{S1}$$

where v_x and D_x, D_z are the velocity and diffusion constants. We stress that the diffusion coefficient of a nanoparticles near a no-slip surface is modified with respect to its bulk value and depends on the distance from the surface relative to the particle radius. Following Ref. [1], the diffusion coefficients are taken as

$$\frac{D_x\,(z)}{D_0} \simeq 1 - \frac{9}{16}\frac{a}{z} + \frac{1}{8}\left(\frac{a}{z}\right)^3 - \frac{45}{256}\left(\frac{a}{z}\right)^4 - \frac{1}{16}\left(\frac{a}{z}\right)^5, \tag{S2a}$$

$$\frac{D_z\,(z)}{D_0} \simeq \frac{6(z-a)^2 + 2(z-a)a}{6(z-a)^2 + 9(z-a)a + 2a^2}, \tag{S2b}$$

where z is the center-of-mass altitude of the particle.

In the experimental setup described in the main text, the particles positions are measured with evanescent-wave microscopy. Thus, particles beyond a certain distance h from the wall are no longer detected. To model this feature of the experiment, we first assume that the initial distribution is localized at a given x position and with a certain initial distribution along z such that $c(x, z, t = 0) = c_{\rm ini}(z)\delta(x)$, where $\delta(x)$ is the Dirac distribution. The range of accessible center-of-mass altitudes is then restricted to the observation zone $z \in [a, h]$, where the lower bound is due to steric interactions. We then only consider the particles that stay in the observation zone in the entire dynamical process. It means that the dynamics is governed by the stochastic process of Eq. (S1), conditioned that the trajectories $z(t') < h$ for time $t' < t$, where t is the observation time. This implies that the concentration field must vanish at the boundary of the observation zone, meaning

$$c(x, z, t) = 0, \quad \text{at} \quad z = H, \tag{S3}$$

which is equivalent to an absorption condition with an infinite absorption rate [2]. The impermeability condition at the wall imposes that the mass flux vanishes, which reads:

$$D_z(z)\left[\frac{\partial c}{\partial z} + \frac{U'_{\rm el}(z)}{kT}c\right] = 0, \quad \text{at} \quad z = a, \tag{S4}$$

where the sphere is in contact with the bottom wall. In practice, the height of the observation zone is typically 500 nm, which is much smaller than the thickness of the overall channel, *i.e.* $20\,\mu$m. The velocity field is therefore approximated with a linear shear flow $v_x(z) = \dot\gamma z$ (schematically indicated in Fig. 1 of the main text and confirmed experimentally in Ref. [3]).

We note that the system considered here is intrinsically out of equilibrium and the number of particles is not conserved. Therefore, the Fokker-Planck equation shown in Eq. (S1) does not have a trivial steady-state solution in contrast with Ref. [4]. Assuming that the concentration vanishes as $|x| \to \infty$ such that $\lim_{x\to\pm\infty} x^\mu \partial_x^\nu c = 0$ for arbitrary integers μ, ν, the moments of the distribution [5] are defined as

$$c_p(z, t) = \int_{\mathbb{R}} x^p c(x, z, t)\,{\rm d}x \quad \text{and} \quad m_p(t) = \int_a^H c_p(z, t)\,{\rm d}z = \bar c_p, \tag{S5}$$

where bar denotes the vertical average $\bar c = \int_a^H c(z){\rm d}z$. Integrating Eq. (S1), one can show that the $p^{\rm th}$ moment follows the recursive equation

$$\left(\frac{\partial}{\partial t} - \frac{\partial}{\partial z}\left(D_z(z)\left[\frac{\partial}{\partial z} + \frac{\phi'(z)}{k_{\rm B}\Theta}\right]\right)\right) c_p(z, t) = p(p-1)D_x(z)c_{p-2}(z, t) + pv_x(z)\,c_{p-1}(z, t). \tag{S6}$$

B. Zeroth moment

Evaluating Eq. (S6) for $p = 0$, we find that the zeroth moment c_0 verifies

$$\left(\frac{\partial}{\partial t} - \frac{\partial}{\partial z}\left(D_z(z)\left[\frac{\partial}{\partial z} + \frac{U'_{\rm el}(z)}{kT}\right]\right)\right) c_0(z,t) = 0, \tag{S7}$$

with an initial condition $c_0(z, t = 0) = c_{\rm ini}(z)$. We search for a separable solution, and inject the ansatz $c_0(z,t) = f(z)\exp(-\lambda t)$ in Eq. (S7). The solutions satisfy

$$\left[\lambda + \frac{\rm d}{{\rm d}z}\left(D_z(z)\left[\frac{\rm d}{{\rm d}z} + \frac{U'_{\rm el}(z)}{kT}\right]\right)\right] f(z) = 0, \tag{S8}$$

together with the boundary conditions

$$D_z(z)\left[\frac{\rm d}{{\rm d}z} + \frac{U'_{\rm el}(z)}{kT}\right] f(z) = 0, \qquad z = a, \tag{S9}$$

$$f(z) = 0, \qquad z = h. \tag{S10}$$

By setting $p(z) = D_z(z)/c_{\rm B}(z)$, $w(z) = 1/c_{\rm B}(z)$ and $q(z) = -[D_z(z)U''_{\rm el}(z) + D'(z)U'_{\rm el}(z)]/c_{\rm B}(z)$, one can show that Eq. (S8), takes the form of a Sturm-Liouville equation [6]

$$-\Big(p(z)f'(z)\Big)' + q(z)f(z) = \lambda w(z) f(z), \tag{S11}$$

where $c_{\rm B}$ is the Boltzmann distribution

$$c_{\rm B}(z) = \frac{\exp\left(-\frac{U_{\rm el}(z)}{kT}\right)}{\int_a^H \exp\left(-\frac{U_{\rm el}(z')}{kT}\right){\rm d}z'}. \tag{S12}$$

Using results from eigenvalue theory, Eq. (S8) has a countable ensemble of solutions $(\lambda_k, f_k(z))_{k\in\mathbb{N}^*}$ that satisfies the boundary conditions Eq. (S9) and (S10), where $0 < \lambda_1 < \lambda_2 < ... < \infty$. The eigenvalues are orthogonal under the definition of the scalar product

$$\langle f, g\rangle = \int_a^H f(z)g(z)w(z)\,{\rm d}z = \int_a^H \frac{1}{c_{\rm B}(z)} f(z)g(z)\,{\rm d}z. \tag{S13}$$

The general solution of Eq. (S7) with its initial condition is

$$c_0(z,t) = \sum_{k\in\mathbb{N}^*} a_{0,k} f_k(z)\exp(-\lambda_k t), \qquad a_{0,k} = \langle c_{\rm ini}, f_k\rangle, \tag{S14}$$

where f_k are taken to be normalized, *i.e.* $\langle f_k, f_k\rangle = 1$. Then integrating Eq. (S14), we find that the total mass of particles, characterized by $m_0(t)$, is given by

$$m_0(t) = \sum_{k\in\mathbb{N}^*} a_{0,k}\overline{f_k}\exp(-\lambda_k t), \tag{S15}$$

and decays over time. The time-dependent altitude probability distribution (see Fig. 3(b) of the main text) are related to the zeroth-moment via

$$\mathcal{P}(z,t) = \frac{\int c(x,z,t){\rm d}x}{\int c(x,z',t){\rm d}x{\rm d}z'} = \frac{c_0(z,t)}{m_0(t)}. \tag{S16}$$

We note that the theoretical initial distribution is normalized, *i.e.* $\int_a^h c_{\rm ini}(z){\rm d}z = 1$, such that the $m_0(t)$ corresponds to the fraction of particles remaining in the observation zone, as plotted in Fig. 3(d) of the main text. The eigenvalue λ_k and eigenfunction f_k are evaluated numerically using a home-made version of the SLEIGN2 code described in Ref. [6].

C. First moment

Evaluating Eq. (S6) for $p = 1$, the governing equation for the first moment c_1 is

$$\left(\frac{\partial}{\partial t} - \frac{\partial}{\partial z}\left(D_z(z)\left[\frac{\partial}{\partial z} + \frac{U'_{\rm el}(z)}{kT}\right]\right)\right) c_1(z,t) = v_x(z)c_0(z,t), \tag{S17}$$

with $c_1(z, t = 0) = 0$. The latter equation can be solved using again the eigenvalue theory [5] and its general solution is of the form

$$c_1(z,t) = \sum_{k\in\mathbb{N}^*} \left(a_{1,k}f_k(z) + a_{0,k}[\zeta_k(z) + \gamma_{1,k}tf_k(z)]\right)\exp(-\lambda_k t) \tag{S18}$$

where ζ_k are the solutions of

$$-\left[\lambda_k + \frac{\mathrm{d}}{\mathrm{d}z}\left(D_z(z)\left[\frac{\mathrm{d}}{\mathrm{d}z} + \frac{U'_{\rm el}(z)}{kT}\right]\right)\right]\zeta_k(z) = \left(v_x(z) - \gamma_{1,k}\right)f_k(z), \tag{S19}$$

with the same boundary conditions as in Eqs. (S9) and (S10). The function ζ_k can be expanded on the basis of f_k as $\zeta_k = \sum_{j\in\mathbb{N}^*} A_{kj}f_j$, such that we can write the solutions as

$$c_1(z,t) = \sum_{k,j\in\mathbb{N}^{*2}} \left[\left(a_{0,k}\gamma_{1,k}t + a_{1,k}\right)\delta_{kj} + a_{0,k}A_{kj}\right]f_j(z)\exp(-\lambda_k t), \tag{S20}$$

where δ_{ij} is the Kronecker symbol. The solvability condition imposes that the right hand side of Eq. (S19) is orthogonal to the functions $f_{j\neq k}$, which implies $\gamma_{1,k} = \langle f_k, v_x f_k\rangle$. Introducing the expansion of ζ_k in Eq. (S19), the matrix coefficients A_{kj} can be evaluated as

$$A_{kj} = -\frac{(1-\delta_{jk})}{\lambda_k - \lambda_j}\langle f_j, v_x f_k\rangle, \tag{S21}$$

where A_{kk} are arbitrary constant and have been set to zero. Finally, the initial condition sets $a_{1,k} = -\sum_{j\in\mathbb{N}^*} a_{0,j}A_{jk}$. Integrating Eq. (S18) vertically, we find the vertical-averaged first moment

$$\begin{aligned} m_1(t) &= \sum_{k\in\mathbb{N}^*}\left[a_{1,k}\overline{f_k} + a_{0,k}\gamma_{1,k}t\overline{f_k} + a_{0,k}\overline{\zeta_k}\right]\exp(-\lambda_k t) \\ &= \sum_{k,j\in\mathbb{N}^{*2}}\left[\left(a_{0,k}\gamma_{1,k}t + a_{1,k}\right)\delta_{kj} + a_{0,k}A_{kj}\right]\overline{f_j}\exp(-\lambda_k t). \end{aligned} \tag{S22}$$

The average distance $\langle x\rangle$ traveled by the particle remaining in the observation zone can be expressed as

$$\langle x\rangle = \frac{\int xc(x,z,t)\,\mathrm{d}x\mathrm{d}z}{\int c(x,z,t)\,\mathrm{d}x\mathrm{d}z} = \frac{m_1(t)}{m_0(t)}, \tag{S23}$$

which allows us to find an closed expression for the average velocity of the particles observed in the channel $\langle V\rangle = \langle x\rangle/t$.

D. Second moment

Considering Eq. (S6) for $p = 2$, the governing partial-differential equation reads

$$\left(\frac{\partial}{\partial t} - \frac{\partial}{\partial z}\left(D_z(z)\left[\frac{\partial}{\partial z} + \frac{U'_{\rm el}(z)}{kT}\right]\right)\right) c_2(z,t) = 2D_x(z)c_0(z,t) + 2v_x(z)c_1(z,t), \tag{S24}$$

with $c_2(z, t = 0) = 0$. The solution of the latter equation is more tedious to find than the solution of the first moment, but it relies on the same method as in the previous section. We seek for solutions of the form:

$$c_2(z,t) = \sum_{k\in\mathbb{N}^*}\left(a_{2,k}f_k(z) + \psi_k(z) + \gamma_{2,k}tf_k(z) + a_{0,k}\gamma_{1,k}t\left[2\zeta_k(z) + \gamma_{1,k}tf_k(z)\right]\right)e^{-\lambda_k t}, \tag{S25}$$

where ψ_k are solution of

$$-\left[\lambda_k + \frac{\mathrm{d}}{\mathrm{d}z}\left(D_z(z)\left[\frac{\mathrm{d}}{\mathrm{d}z} + \frac{U'_{\mathrm{el}}(z)}{kT}\right]\right)\right]\psi_k(z) = 2a_{0,k}D_x(z)f_k(z) - \gamma_{2,k}f_k(z) + 2\left(a_{1,k}v_x(z)f_k(z) + a_{0,k}(v_x(z) - \gamma_{1,k})\zeta_k(z)\right), \tag{S26}$$

with the boundary conditions Eqs. (S9) and (S10). Here again, we expand ψ_k in the basis of f_j, *i.e.* $\psi_k(z) = \sum_{j=1}^{\infty} B_{kj}f_j(z)$, and find the corresponding coefficients using the solvability condition and initial condition as

$$\gamma_{2,k} = 2a_{0,k}\langle f_k, D_x f_k\rangle + 2a_{1,k}\langle f_k, v_x f_k\rangle + 2a_{0,k}\langle f_k, (v_x - \gamma_{1,k})\zeta_k\rangle \tag{S27a}$$

$$B_{kj} = -\frac{(1-\delta_{jk})}{\lambda_k - \lambda_j}\left[2a_{0,k}\langle f_j, D_x f_k\rangle + 2a_{1,k}\langle f_j, v_x f_k\rangle + 2a_{0,k}\langle f_j, (v_x - \gamma_{1,k})\zeta_k\rangle\right] \tag{S27b}$$

$$a_{2,k} = -\sum_{j\in\mathbb{N}^*} B_{jk} \tag{S27c}$$

Integrating Eq. (S25) across the observation area, we can find the vertical-averaged second moment

$$\begin{aligned} m_2(t) &= \sum_{k\in\mathbb{N}^*}\left(a_{2,k}\overline{f_k} + \overline{\psi_k} + \gamma_{2,k}t\overline{f_k} + a_{0,k}\gamma_{1,k}t\left[2\overline{\zeta_k} + \gamma_{1,k}t\overline{f_k}\right]\right)e^{-\lambda_k t} \\ &= \sum_{k,j\in\mathbb{N}^{*2}}\left[\left(a_{2,k} + \gamma_{2,k}t + a_{0,k}\gamma_{1,k}^2t^2\right)\delta_{kj} + 2a_{0,k}\gamma_{1,k}A_{k,j}t + B_{k,j}\right]\overline{f_j}e^{-\lambda_k t}. \end{aligned} \tag{S28}$$

The variance of the distribution in the streamwise direction is defined as

$$\langle (x - \langle x\rangle)^2\rangle = \frac{\int x^2 c(x,z,t)\,\mathrm{d}x\mathrm{d}z}{\int c(x,z,t)\,\mathrm{d}x\mathrm{d}z} - \left(\frac{\int xc(x,z,t)\,\mathrm{d}x\mathrm{d}z}{\int c(x,z,t)\,\mathrm{d}x\mathrm{d}z}\right)^2, \tag{S29}$$

such that the dispersion coefficient reads

$$\mathcal{D}_x = \frac{\langle (x - \langle x\rangle)^2\rangle}{2t} = \frac{1}{2t}\left(\frac{m_2(t)}{m_0(t)} - \frac{m_1^2(t)}{m_0^2(t)}\right). \tag{S30}$$

E. Long-time asymptotic expression

As shown above, the moments of the concentration field are found to follow a modal decomposition $c_p(z,t) = \sum_{k=1}^{\infty} c_{p,k}(z,t)\exp(-\lambda_k t)$, where $c_{p,k}$ are polynomial functions of t of degree p, and where $0 < \lambda_1 < \lambda_2 < \cdots$. Therefore, there is no steady-state solution and the concentration fields decays to zero at long times. Nevertheless, in the long-time limit, the concentration is governed by the slowest relaxation mode λ_1, and the probability density function of particles remaining in the channel converges toward a steady state. For time larger than $t \gg \frac{1}{\lambda_2 - \lambda_1}$, we truncate the expansion to its leading order and the moments $c_{p\leq 2}$ follow

$$c_0(z,t) \simeq a_{0,1}f_1(z)e^{-\lambda_1 t}, \tag{S31}$$

$$c_1(z,t) \simeq \left(a_{1,1}f_1(z) + a_{0,1}[\zeta_1(z) + t\gamma_{1,1}f_1(z)]\right)e^{-\lambda_1 t}, \tag{S32}$$

$$c_2(z,t) \simeq \left(a_{2,1}f_1(z) + \psi_1(z) + t\gamma_{2,1}f_1(z) + ta_{0,1}\gamma_{1,1}\left[2\zeta_1(z) + t\gamma_{1,1}f_1(z)\right]\right)e^{-\lambda_1 t}. \tag{S33}$$

Similarly, the vertical-averaged moments can be truncated to

$$m_0(t) \simeq a_{0,1}\overline{f_1}e^{-\lambda_1 t}, \tag{S34}$$

$$m_1(t) \simeq \left(a_{1,1}\overline{f_1} + a_{0,1}[\overline{\zeta_1} + t\gamma_{1,1}\overline{f_1}] \right) e^{-\lambda_1 t}, \tag{S35}$$

$$m_2(t) \simeq \left(a_{2,1}\overline{f_1} + \overline{\psi_1} + t\gamma_{2,1}\overline{f_1} + ta_{0,1}\gamma_{1,1}\left[2\overline{\zeta_1} + t\gamma_{1,1}\overline{f_1}\right] \right) e^{-\lambda_1 t}. \tag{S36}$$

Introducing the latter expansion into Eq. (S16), the long-time altitude probability distribution converges toward a steady state, independent of the initial distribution and is given by

$$\mathcal{P}(z) = \frac{f_1(z)}{\overline{f_1}}, \tag{S37}$$

as observed in Fig. 3(b) of the main text. The average velocity of the particles observed in the channel also converges toward a finite value given by

$$\langle V \rangle = \frac{\langle x \rangle}{t} = \langle f_1, v_x f_1 \rangle = \int_a^h \frac{1}{c_{\mathrm{B}}(z)} f_1^2(z) v_x(z)\, \mathrm{d}z. \tag{S38}$$

The averaging here corresponds to a time average of the velocity as $\langle V \rangle = \frac{1}{t}\int_0^t v_x(z_t)\,\mathrm{d}t$, where z_t denotes the vertical position at time t. Interestingly, the long-time asymptotic time-average velocity of particle $\langle x \rangle / t$ differs from the ensemble-average velocity $\langle v_x \rangle$ of particles remaining in the channel, which reads

$$\langle v_x \rangle = \int_a^h \mathcal{P}(z) v_x(z)\, \mathrm{d}z = \int_a^h \frac{f_1(z)}{\overline{f_1}} v_x(z)\, \mathrm{d}z. \tag{S39}$$

One would expect the two averaged velocities defined in Eqs. (S38) and (S39) to be the same from the ergodic theorem. Such a principle holds in equilibrium physics and the difference in the long-time velocity arises from the nonequilibrium nature of the problem. Finally the long-time dispersion coefficient can be computed from Eq. (S30) as

$$\mathcal{D}_x = \langle f_1, D_x f_1 \rangle + \langle f_1, (v_x - \langle V \rangle)\zeta_1 \rangle = \int_a^h \frac{1}{c_{\mathrm{B}}(z)} f_1^2(z) D_x(z)\, \mathrm{d}z + \int_a^h \frac{1}{c_{\mathrm{B}}(z)} (v_x(z) - \langle V \rangle)\zeta_1(z) f_1(z)\, \mathrm{d}z. \tag{S40}$$

which corresponds to the Eq. (4) of the main text.

F. Tracer non-interacting particles

Here, we focus on the limit of point-like particles when the radius of the particle is small with respect to the channel size, *i.e.* $a/h \to 0$. The typical length scale of variation of the diffusion constant due to the hydrodynamic interactions is given by the radius of the particle such that we neglect the spatial variation of D_x and D_z. Furthermore, we ignore here the effect external forces, meaning that $U_{\mathrm{el}}(z) = 0$. In that case, the Eq. (S8) simplifies and can be computed exactly with its boundary condition Eqs. (S9) and (S10). The first mode is described by

$$\lambda_1 = \frac{\pi^2 D_0}{4h^2}, \qquad f_1(z) = \frac{\sqrt{2}}{h} \cos\left(\frac{\pi z}{2h}\right), \qquad c_{\mathrm{B}}(z) = \frac{1}{h}. \tag{S41}$$

Using this expression in Eq. (S40), we can compute exactly the steady-state average velocity and dispersion coefficient

$$\langle V \rangle = \frac{\dot{\gamma} h}{2}\left(1 - \frac{2}{\pi^2}\right) \approx 0.29736\, \dot{\gamma} h, \qquad \mathcal{D}_x = D_0 + \frac{240 - 12\pi^2 - \pi^4}{3\pi^6} \frac{\dot{\gamma}^2 h^4}{4D_0} \approx D_0\left(1 + 0.0083753\ \mathrm{Pe}^2\right). \tag{S42}$$

This latter result can be compared, as in Fig. 4(b) of the main text, to the classical, Taylor-Aris tracer result for reflecting boundaries on both the top and bottom of the channel. Recalling the discussion preceding Eq. (1) of the main text, the Taylor-Aris result is $\mathcal{D}_x^{\mathrm{TA}} = D_0\left(1 + 30^{-1}\ \mathrm{Pe}^2\right)$.

G. Dispersion coefficient in a 2d channel with reflecting boundary condition

The long-time dispersion coefficient in the case of a channel of size h with reflecting boundary conditions at both interfaces can be found in Refs. [4, 7] and takes the form

$$\mathcal{D}_x = \bar{D}_x + \int_a^h \frac{1}{D_z(z) c_{\mathrm{B}}(z)} \left[\int_a^z \left[v_x\left(z'\right) - \langle V \rangle \right] c_{\mathrm{B}}\left(z'\right) \mathrm{d}z' \right]^2 \mathrm{d}z \ , \tag{S43}$$

where the long-time averaged velocity is here $\langle V \rangle = \int_a^h c_{\mathrm{B}}(z) v_x(z) \, \mathrm{d}z$.

MODEL SCHEMATICS

In Figure S1 we recall the models used to predict dispersion in a simple shear flow. As shown in Fig. 2(a), this dispersion depends on experimental variations of the salt concentration (particle-wall interaction) and the laser power (variation of the effective channel height) in the evanescent-wave microscopy observations reported here. Shown in the first column of Figure S1 are schematics describing

- (a) the classical Taylor prediction [8, 9], with tracer particles and reflection conditions at the boundaries;
- (b) a model with no particle consumption, but with one interacting wall (potential and hydrodynamic interactions), derived from Refs. [4, 7] and seen in Eq. S43;
- (c) a model considering tracer particles with a consumption condition at one wall, Eq. S42;
- and (d) the full model as Eq. 4 in the main text and derived above, also in Eq. S40.

For convenience, the line styles of Fig. 4 and the dispersion equations are also recalled.

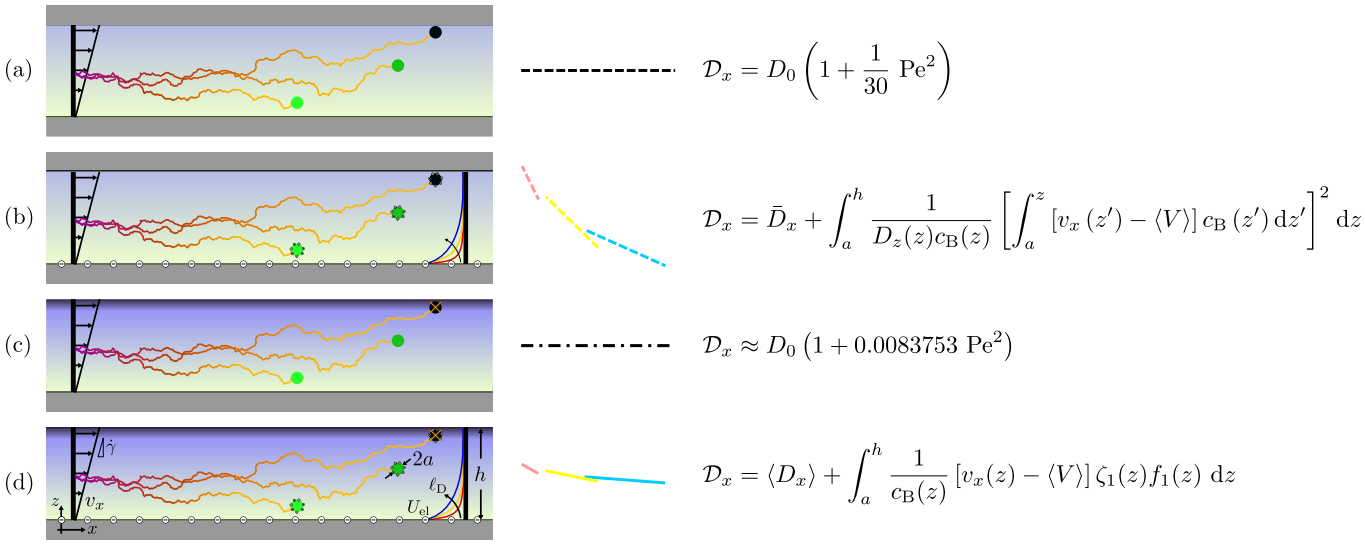

Figure S1. Schematics (left column); line style of Fig. 4 of the main text (central column); and dispersion predicition (right column) for the different models described in the text.

VIDEO DESCRIPTIONS

- In Video S1 is shown a typical TIRFM image sequence with superimposed particle trajectories obtained with in-house particle-tracking software based on the `regionprops` function of MATLAB . The pressure imposed across the microfluidic system was 40 mbar with 150 mW laser illumination. The NaCl concentration was 5.4 mg/mL and delay times are indicated.
- As shown in the snapshots of Fig. 1(b), Video S2 displays the same data in Video S1, with the origins of the displayed particles' trajectories at a common point; a sample of 62 particles from each ensemble was used.

[1] Zhenzhen Li, Loïc D'eramo, Choongyeop Lee, Fabrice Monti, Marc Yonger, Patrick Tabeling, Benjamin Chollet, Bruno Bresson, and Yvette Tran, "Near-wall nanovelocimetry based on total internal reflection fluorescence with continuous tracking," Journal of Fluid Mechanics **766**, 147–171 (2015).

[2] Rudro R Biswas and Pabitra N Sen, "Taylor dispersion with absorbing boundaries: A stochastic approach," Physical review letters **98**, 164501 (2007).

[3] Alexandre Vilquin, Vincent Bertin, Pierre Soulard, Gabriel Guyard, Elie Raphaël, Frédéric Restagno, Thomas Salez, and Joshua D. McGraw, "Time dependence of advection-diffusion coupling for nanoparticle ensembles," Phys. Rev. Fluids **6**, 064201 (2021).

[4] Howard Brenner and Lawrence J Gaydos, "The constrained brownian movement of spherical particles in cylindrical pores of comparable radius: models of the diffusive and convective transport of solute molecules in membranes and porous media," Journal of Colloid and Interface Science **58**, 312–356 (1977).

[5] NG Barton, "An asymptotic theory for dispersion of reactive contaminants in parallel flow," The ANZIAM Journal **25**, 287–310 (1984).

[6] Paul B Bailey, William N Everitt, and Anton Zettl, "The sleign2 sturm-liouville code," ACM Trans. Math. Software **27**, 143–192 (2001).

[7] Arthur Alexandre, Thomas Guérin, and David S Dean, "Generalized taylor dispersion for translationally invariant microfluidic systems," Physics of Fluids **33**, 082004 (2021).

[8] Geoffrey Ingram Taylor, "Dispersion of soluble matter in solvent flowing slowly through a tube," Proceedings of the Royal Society of London. Series A. Mathematical and Physical Sciences **219**, 186–203 (1953).

[9] Rutherford Aris, "On the dispersion of a solute in a fluid flowing through a tube," Proceedings of the Royal Society of London. Series A. Mathematical and Physical Sciences **235**, 67–77 (1956).